

## First Production of Intense Circularly Polarized Hard X Rays from a Novel Multipole Wiggler in an Accumulation Ring

Shigeru Yamamoto, Hiroshi Kawata, Hideo Kitamura, and Masami Ando

*Photon Factory, National Laboratory for High Energy Physics, Oho, Tsukuba, Ibaraki 305, Japan*

Nobuhiko Saki and Nobuhiro Shiotani

*Institute of Physical and Chemical Research, Wako, Saitami 351-01, Japan*

(Received 21 February 1989)

A novel multipole wiggler and an associated beam line have been installed in the accumulation ring for the TRISTAN project at the National Laboratory for High Energy Physics (KEK). An intense source of circularly polarized synchrotron radiation with energy ranging from 40 to 80 keV has been achieved for the first time. The degree of circular polarization  $P_c \cong 0.7$  at 60 keV of photon energy was in good agreement with a theoretical prediction for the 6-GeV operation of the accumulation ring.

PACS numbers: 42.72.+h, 07.60.Fs, 41.70.+t, 75.25.+z

For intensive studies on magnetic materials, it has been widely known that extensive use of circularly polarized x-ray photons is quite essential and important. However, for a long time only a very weak  $\gamma$ -ray source has been used in the x-ray region.<sup>1,2</sup> Recent attempts to use circularly polarized synchrotron radiation, either from off the electron orbital plane<sup>3</sup> or produced by a phase plate<sup>4</sup> for a magnetic Compton-scattering experiment, still suffer from a lack of intensity. In order to overcome this situation a novel multipole wiggler proposed by Yamamoto and Kitamura<sup>5</sup> was constructed<sup>6</sup> and has been installed together with an associated beam line<sup>7</sup> in the accumulation ring (AR) for the TRISTAN project at the National Laboratory for High Energy Physics (KEK). Here we report the results of the first operation of the multipole wiggler for the production of circularly polarized hard x rays.

The wiggler has horizontal and vertical pairs of permanent magnet arrays of NdFeB alloy in the pure Halbach-type configuration<sup>8</sup> as shown in Fig. 1 (number of periods  $N=21$ , and periodicity  $\lambda_u=16$  cm). One pair generates a sinusoidal magnetic field with a phase difference of  $\pm\pi/2$  relative to the other. The peak field strength, which is controllable by changing the magnet gap, ranges up to 2 kG for the horizontal field,  $B_{x0}$ , and up to 9.7 kG for the vertical one,  $B_{y0}$ . Thus the total magnetic field,  $\mathbf{B}$ , can be described as their superposition,

$$\mathbf{B} = \mathbf{e}_x B_{x0} \sin \left[ \frac{2\pi z}{\lambda_u} \pm \frac{\pi}{2} \right] - \mathbf{e}_y B_{y0} \sin \left[ \frac{2\pi z}{\lambda_u} \right], \quad (1)$$

where  $\mathbf{e}_x$  and  $\mathbf{e}_y$  are the unit vectors in the horizontal  $x$  and vertical  $y$  directions, respectively, while  $z$  is taken along the axis of the wiggler. The field  $\mathbf{B}$  given by Eq. (1) produces a deformed-helix motion of the electrons. Hereafter we will abbreviate the multipole wiggler as EMPW, since an *elliptic* motion of an electron should be

observed about the axis. The rotation direction of the helix can be reversed by selecting the phase difference between the vertical and horizontal pairs as either  $\pi/2$  or  $-\pi/2$ . The  $K$  parameter which characterizes the radiation from EMPW is defined in the  $x$  and  $y$  directions as

$$K_{x(y)} = 9.34 \times 10^{-5} B_{x0(y)0} \lambda_u, \quad (2)$$

with  $B$  given in units of G and  $\lambda$  in cm. In the present case,  $K_x$  ranges up to 3, and  $K_y$  up to 15.

A relativistic electron in the field given by Eq. (1) produces radiation with several thousand harmonics<sup>5</sup> having quasicircular polarization over a wide energy range. The generation of higher-order harmonics is due to an elliptic deformation from a completely helical trajectory of the electron, whereas only the first harmonic is obtained from the helical wiggler.<sup>9</sup> These higher harmonics lead to the use of the radiation in a high-energy region. Especially, the radiation for  $K_y \gg 1$  and  $K_x \sim 1$  (designated as "wiggler radiation") has a spectrum extending to 80 keV<sup>6</sup> when EMPW is coupled with the 6-GeV storage ring, and can be explained as a superposition of the off-

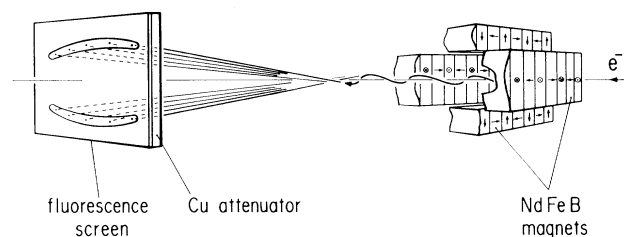


FIG. 1. Schematic illustration of the present multipole wiggler (EMPW). Arrows on the individual magnets denote their magnetization directions. A relativistic electron draws an orbit of a deformed helix (Ref. 5). A fluorescence screen with a Cu attenuator is also shown to confirm the radiation from the expected orbit.

plane radiation from a bend source. This is because each half period of the sinusoidal orbit due to the vertical field can be regarded as the arc in a bending magnet, and is tilted up or down alternately by the horizontal field by the angle  $K_x/\gamma$ , where  $\gamma$  is the relativistic energy of the electron. The angular flux density,  $\mathcal{D}$ , which is defined here as the photon flux per unit solid angle and stored current in the ring, and the degree of circular polarization,  $P_c$ , can be obtained with this bend-source approximation<sup>6</sup> for the wiggler radiation.

Immediately after the commissioning of EMPW (e.g., optimization of the electron orbit in the ring), the radiation in the hard-x-ray region with  $K_y = 15$  was characterized at the beam line BL NE1 (Ref. 7) in the 6-GeV operation of AR. Figure 2 shows the first direct observation of photons produced by EMPW. It is an image projected on a fluorescence screen right after a Cu attenuator with a thickness of 7 mm placed at 35 m from EMPW. Since the highest-energy portion of the photons is radiated along the tangential direction from the orbit, the bright line on the fluorescence screen is a locus of in-

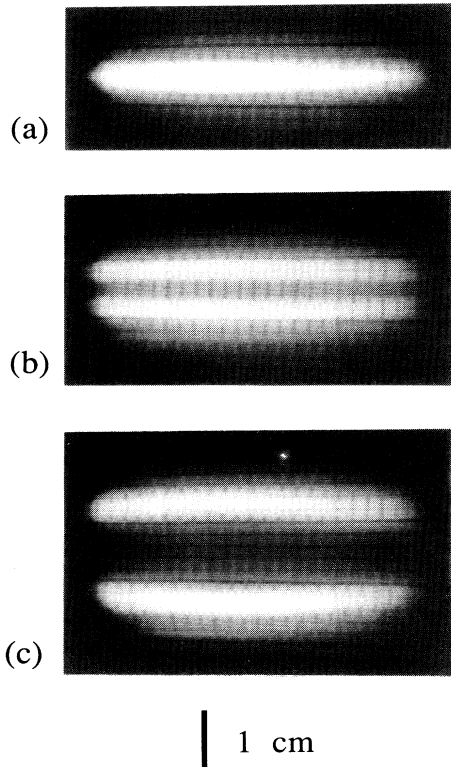


FIG. 2. Images on the fluorescence screen with  $K_y = 15$ ; (a)  $K_x = 0$ , (b)  $K_x = 1.3$ , and (c)  $K_x = 3.0$ , with the stored current of 0.5 mA. Fattening of the bright pattern on the screen from a single segment (a) to ellipses (b) and (c) corresponds to variation of an electron orbit from a plane sinusoidal type to a deformed-helix type with the increasing horizontal field  $B_{x0}$ . The elliptically polarized radiation is obtained on the axis, where it is interrupted by a Cu attenuator.

tersections of the orbital tangent and the screen. Therefore, the radiation obtained on the bright line has linear polarization, and the circular polarization of the radiation inside the bright elliptic line has an opposite sense to that outside the line. The elliptic patterns on the screen [Figs. 2(b) and 2(c)] prove that the electron orbit forms a deformed helix when the horizontal magnetic field is applied. The reason why the pattern is not a complete ellipse but separated into upper and lower parts is that the energy radiated towards the missing parts of the ellipse is not high enough to penetrate the Cu attenuator, since the vertical magnetic field at the corresponding point on the electron orbit is not so strong. Fattening of the elliptic pattern with increasing  $K_x$  shows the variation of the electron orbit from a plane sinusoidal type (i.e., an orbit in the usual plane multipole wiggler/undulator with vertical field only) to a deformed-helix type. In the present study the case with  $K_x = K_y \leq 3$  is not shown, since an appropriate attenuator for the radiation for this case was not available.

The quantitative evaluation of  $P_c$  and  $\mathcal{D}$  was made by Compton-scattering measurements with a magnetized polycrystalline Fe specimen. The measuring system for the evaluation is substantially the same as that used by Sakai, Terashima, and Sekizawa.<sup>10</sup> The radiation monochromatized by Ge 400 Bragg diffraction, was directed to the specimen inserted in an electromagnet which controls the spin vector,  $\mathbf{S}$ , of the Fe specimen. The Compton-scattered x rays were detected by a Ge solid-state detector.  $P_c$  can be derived from the equation given by Lipps and Tolhoek,<sup>11</sup>

$$P_c = \frac{I^+ - I^-}{I^+ + I^-} \left( \frac{n^\uparrow - n^\downarrow}{n^\uparrow + n^\downarrow} \right)^{-1} \frac{\Phi_0(E_0, \theta)}{\Phi_{\text{spin}}(E_0, \theta, \mathbf{S}, \mathbf{K}_0, \mathbf{K})}, \quad (3)$$

where  $I^+$  and  $I^-$  denote the intensities of scattered x rays from the specimen magnetized up ( $\mathbf{S}$ ) and down ( $-\mathbf{S}$ ), respectively.  $n^\uparrow$  and  $n^\downarrow$  are the averaged electron numbers of the spin-up state and spin-down state, respectively.  $\Phi_{\text{spin}}$  and  $\Phi_0$  are the spin-dependent and ordinary Compton-scattering cross sections, respectively.  $E_0$  is the incident x-ray energy and  $\theta$  is the scattering angle between  $\mathbf{K}_0$ , the wave vector of the incident x ray, and  $\mathbf{K}$ , that of the scattered one.  $P_c$  is evaluated by the measured  $I^+$  and  $I^-$  with the value of  $(n^\uparrow - n^\downarrow)/(n^\uparrow + n^\downarrow) = 0.080$  (Ref. 12) since  $\Phi_0$  and  $\Phi_{\text{spin}}$  are well known, whereas  $\mathcal{D}$  is evaluated by  $(I^+ - I^-)/2$ . The sense of either right- or left-handed circular polarization should be able to be predicted based on the electron trajectory deduced from the magnetic field of Eq. (1). The prediction was confirmed using Eq. (3) while changing the phase difference.

Figure 3 shows the dependences of  $P_c$  and  $\mathcal{D}$  of the wiggler radiation on the vertical observation angle  $\Psi$  in the cases of (a)  $K_x = 1$  and (b)  $K_x = 1.5$  with  $K_y$  fixed at 15. The radiation for these cases (critical energy = 24 keV) is characterized at 60 keV, since the magnetic

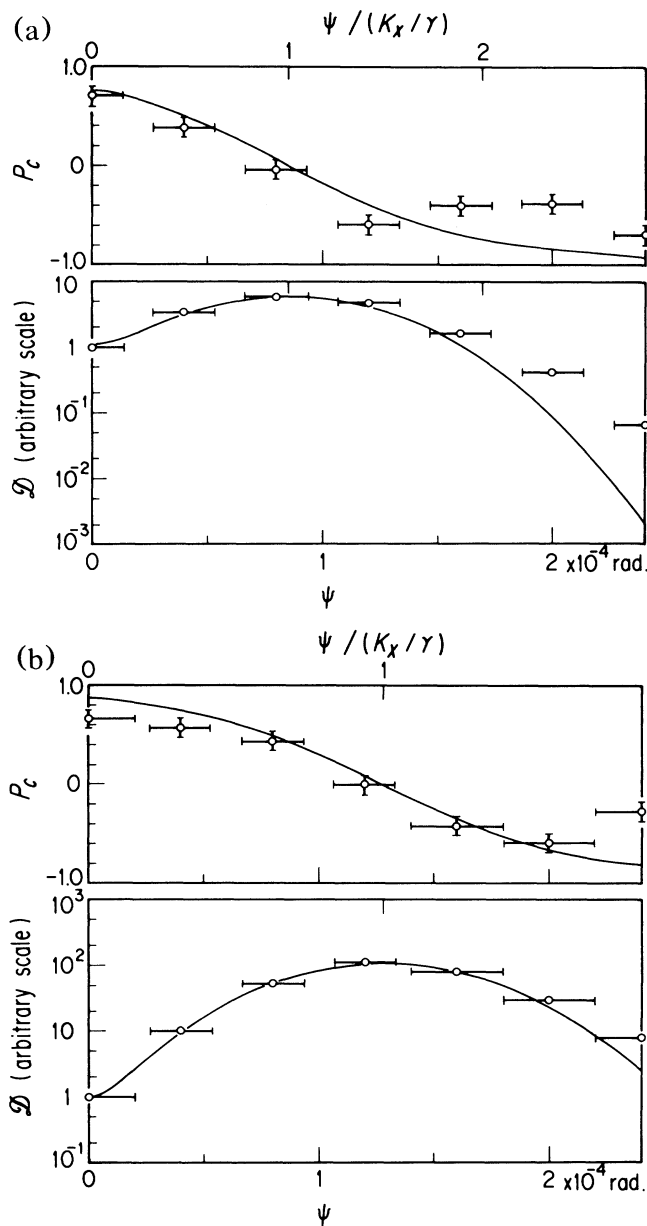


FIG. 3. The dependences of the degree of circular polarization,  $P_c$ , and the angular flux density,  $\mathcal{D}$ , of the radiation at 60 keV on the vertical observation angle,  $\Psi$ , in the cases of (a)  $K_x = 1$  and (b)  $K_x = 1.5$  with  $K_y = 15$  with the stored current of 5–20 mA. Circles denote the values measured with the vertical aperture given by the horizontal bar and the horizontal aperture fixed at  $2 \times 10^{-4}$  rad. Solid curves represent the results of a calculation in which we consider the vertical divergence of the electron beam with the bend-source approximation (Ref. 6). The aperture of the incident slit and the source depth of EMPW are also taken into account. The calculated flux density is compared with the measured one with an arbitrary scale. They are normalized at  $\Psi = 8 \times 10^{-5}$  rad to have the same value. The circular polarization changes its sense at  $\Psi = K_x / \gamma$ , since the radiation obtained on the bright line corresponds to that emitted along the direction of  $\Psi = K_x / \gamma$  (Fig. 2).

Compton scattering of the transition metals, which requires photon energy above 50 keV, is intended as the first practical application of the radiation. The angle  $\Psi$  is set by scanning the incident slit in the vertical direction. Solid curves represent the results of a calculation under the bend-source approximation,<sup>6</sup> in which we consider the vertical angular spread of the electron beam,  $\sigma_{y'} = 2.2 \times 10^{-5}$  rad,<sup>13</sup> in AR, the aperture of the incident slit, and the source depth of EMPW. The selection of the values of  $K_x$  in this study was made under the following conditions: (1)  $K_x \gg \gamma \sigma_{y'}$  and  $K_x \gtrsim 1$  for achievement of high  $P_c$ ; (2)  $K_x \lesssim 1$  for achievement of high  $\mathcal{D}$ . The fact that AR has a low  $\gamma \sigma_{y'}$  of 0.26 enables the above selection of  $K_x$ .  $\mathcal{D}$  is shown on an arbitrary scale, since the absolute spectral measurements have not been performed yet.

As seen from Fig. 3, EMPW has the following remarkable features. (1) It can generate highly circularly polarized radiation of  $P_c \cong 0.7$  at an energy of 60 keV in the horizontal plane. (2) Its angular flux density is very high: The in-plane  $\mathcal{D}$  ranges from a tenth for  $K_x = 1$  to a hundredth for  $K_x = 1.5$  of its maximum at  $\Psi = K_x / \gamma$ . The maximum is at least 20 times higher than that from a 10 kG bending magnet in AR. Small discrepancies between the experiment and the calculation of  $P_c$  and  $\mathcal{D}$  at  $\Psi \geq 2K_x / \gamma$  are probably due to stray x rays. But this is not crucial in experiments because utilization of the radiation is made on the axis. Thus it should be emphasized that such intense circularly polarized radiation will certainly stimulate research on the interaction between x rays and the spin state of electrons in condensed matter.

We would like to express our sincere thanks to Y. Kimura and the staff of the TRISTAN accelerator group for allowing us unlimited access to AR and fine machine operation for the present work. S. Asaoka, A. Iida, T. Iwazumi, N. Kanaya, Y. Kitajima, A. Mikuni, T. Miyahara, M. Sato, S. Sato, and T. Shioya of the Photon Factory, KEK; F. Itoh, H. Sakurai, and T. Sugawa of the Institute for Materials Research, Tohoku University; S. Nanao, Y. Sakurai, and Y. Tanaka of the Institute of Industrial Science, The University of Tokyo; and M. Itoh and O. Mao of the Institute of Physical and Chemical Research are thanked for their collaboration in performing experiments.

<sup>1</sup>N. Sakai and K. Ono, Phys. Rev. Lett. **37**, 351 (1976).

<sup>2</sup>N. Sakai and H. Sekizawa, Phys. Rev. B **36**, 2164 (1987).

<sup>3</sup>M. J. Cooper, D. Laundry, D. A. Cardwell, D. N. Timms, and R. S. Holt, Phys. Rev. B **34**, 5984 (1986).

<sup>4</sup>D. M. Mills, Phys. Rev. B **36**, 6178 (1987).

<sup>5</sup>S. Yamamoto and H. Kitamura, Jpn. J. Appl. Phys. **26**, L1613 (1987).

<sup>6</sup>S. Yamamoto, T. Shioya, S. Sasaki, and H. Kitamura, Rev. Sci. Instrum. (to be published).

<sup>7</sup>H. Kawata, T. Miyahara, S. Yamamoto, T. Shioya, H. Kitamura, S. Sato, S. Asaoka, N. Kanaya, A. Iida, A. Mikuni, M. Sato, T. Iwazumi, Y. Kitajima, and M. Ando, *Rev. Sci. Instrum.* (to be published).

<sup>8</sup>K. Halbach, *Nucl. Instrum. Methods* **187**, 109 (1981).

<sup>9</sup>B. M. Kincaid, *J. Appl. Phys.* **48**, 2684 (1977).

<sup>10</sup>N. Sakai, O. Terashima, and H. Sekizawa, *Nucl. Instrum. Methods Phys. Res., Sect. B* **221**, 419 (1984).

<sup>11</sup>F. W. Lipps and H. A. Tolhoek, *Physica (Utrecht)* **20**, 395 (1954).

<sup>12</sup>In this study, we used the values of  $n^+ - n^- = 2.0$  and

$n^+ + n^- = 25$ , considering the reduction of  $n^+ - n^-$  due to the insufficient magnetization of the specimen from the reported value of 2.2 [cf. C. Kittel, *Introduction to Solid State Physics* (Wiley, New York, 1976), 5th ed.] and the reduction of  $n^+ + n^-$  due to the broad energy spectrum of the Compton-scattered x rays from the atomic number of Fe of 26.

<sup>13</sup>S. Kamada (private communication). The present 6-GeV operation of AR is made with horizontal and vertical beam emittances of  $\epsilon_x = 2.5 \times 10^{-7}$  m rad and  $\epsilon_y = 2.0 \times 10^{-9}$  m rad, respectively, and betatron functions at the center of EMPW of  $\beta_{x,y} = 4$  m

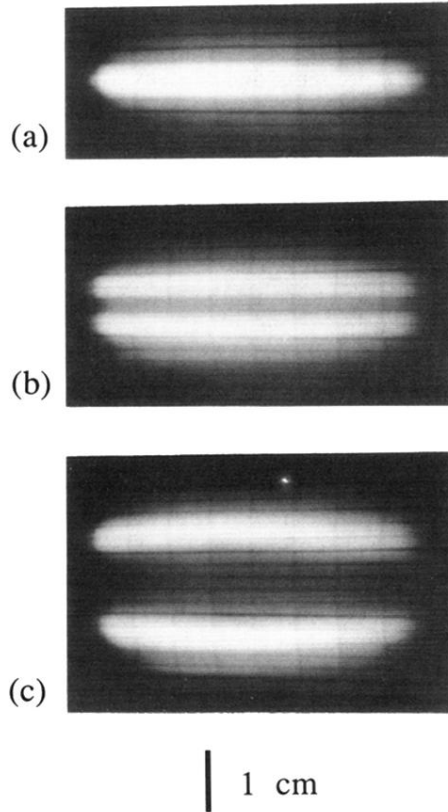


FIG. 2. Images on the fluorescence screen with  $K_y = 15$ ; (a)  $K_x = 0$ , (b)  $K_x = 1.3$ , and (c)  $K_x = 3.0$ , with the stored current of 0.5 mA. Fattening of the bright pattern on the screen from a single segment (a) to ellipses (b) and (c) corresponds to variation of an electron orbit from a plane sinusoidal type to a deformed-helix type with the increasing horizontal field  $B_{x0}$ . The elliptically polarized radiation is obtained on the axis, where it is interrupted by a Cu attenuator.